Journal of ELECTRICAL ENGINEERING, VOL 61. NO 7/s, 2010, 133-136

STRAY FIELD MEASUREMENT DURING POWER TRANSFORMER ENERGIZING

Miroslav Novák*

This work verifies the significance of the transformer primary stray field to the inrush current magnitude. This study is presented computational method derived from a well-known published formula related to deep saturation of the transformer core. The results of the numerical model based on the theoretical analysis are compared to measurements for four winding configurations. The axial component of the magnetic field in the transversal gap of coils is presented during the transformer energizing.

Keywords: transformer, inrush current, magnetic stray field

1 INTRODUCTION

The transformer energizing is a transient phenomenon influenced by the core saturation due to remanent flux which does not correspond to the prospective flux in transformer steady state of operation [1]. The excessive inrush current can blow fuses, weld contactors or even damage transformer winding [2]. Unfortunately, modern transformer core material and designs with high operational working flux lead to the high inrush current.

The peak value of the first cycle of inrush current is an important entry for transformer usage and should be a part of proper transformer design. There are several methods for calculating it. A simple method based on deep saturation analysis [3]. The importance of primary impedance is mentioned in works [4, 5]. Advanced method of the inrush current computation uses transformer numerical models with simple implementation of non-linear inductor [6, 7] or more advanced models with hysteresis [8].

2 THEORY

The proposed method is derived from the saturation analysis [3] with consideration of the magnetic core nonlinearity in this study. The secondary winding is omitted for a simplification.

The transformer is supplied by sinusoidal AC voltage

$$u(t) = U\sin(\omega t + \theta), \tag{1}$$

where U is primary voltage magnitude, ω is angular frequency and θ is angle corresponding to the switching on instant.

The magnetic flux $\phi(t)$ consists of an alternating flux driven by the electromotive force ε by Faraday's law, with consideration of the voltage drop $iR = i(R_p + R_{net})$, and constant remanent flux Φ_r, which is present in the core before the switching on

$$\phi(t) = -\frac{1}{n}\int_0^t \varepsilon dt + \Phi_r = -\frac{1}{n}\int_0^t (u - iR)dt + \Phi_r . \tag{2}$$

where R_p - is the primary coil resistance, R_{net} - is the power source plus leads resistance, n - is the number of primary coil turns and i - is the primary current.

The flux of primary coil ϕ divides between the transformer core ϕ_c and the air gap between the core and the winding ϕ_g

$$\phi = \phi_c + \phi_g = B_c A_c + B_g A_g = B_c A_c + \mu_0 H A_g , \tag{3}$$

where A_c is the core cross-section area and A_g is the air gap area. The primary coil transversal cross-section area $A_p = A_c + A_g$. The flux density in the air gap is simply $B_g = \mu_0 H$, where μ_0 is the vacuum permeability. The core magnetic flux density B_c is then

$$B_c = \frac{1}{A_c}\left(\phi(t) - \mu_0 H(t) A_g\right). \tag{4}$$

The magnetic field intensity $H(B_c)$ is obtained either by interpolation from the anhysteretic magnetizing curve or from the hysteresis loop model. The data of anhysteretic curve just as an implementation of the Jiles-Atherton hysteresis loop model were published in [10]. The data of anhysteretic curve in [10] was taken on the same transformer sample as for this article.

Finally the primary current is calculated from Ampère's circuital law

$$i(t) = \frac{l(t)}{n} H(t), \tag{5}$$

where l is an average length of flux lines which vary from the magnetic circuit length l_c to the height of the coil winding l_w

$$l = l_c s + l_w (1 - s), \tag{6}$$

where s is saturation coefficient $s = \phi_c/(\phi_c - \phi_g)$.
The coil inductance during saturation behaves as an air coil, therefore the height of the coil winding l_w is used as in case of long solenoid.

Transformer design affects the inrush current in several ways. The construction and material of the transformer core are determinative for the hysteresis loop. Conventional Fe-Si electrical steel has saturation level B_s at about 2 T, so the reduction of the nominal working magnetic flux B improve reserve to saturation and reduces the inrush current. The remanent flux density B_r is mainly dependent on the joints overlapping.

The winding diameter determinates simultaneously the primary coil cross-section A_p and the resistance R_p.

* Institute of Mechatronics and Computer Engineering, Technical University of Liberec, Faculty of Mechatronics, Informatics and Interdisciplinary Studies, Studentská 2, 461 17 Liberec, Czech Republic; miroslav.novak@tul.cz

ISSN 1335-3632 © 2010 FEI STU

The importance of the winding diameter for the inrush current suppression is solved also in [9].

3 MEASUREMENTS

Two UI core transformers 1.2 kVA, 230/230 V, 50 Hz were made with concentric coils divided in two halves for each limb. 6 mm air gaps in the centre of coils were left in for the purpose of the stray field measurement. Each transformer was designed with different coil diameters built up by plastic spacers, see Table 1. The coil distance from the core limb was measured by a slide gauge in air gap and calculated from measured wire resistance. All coils have the same number of turns. The outer as well as the inner coil was used as the primary winding, so a set of four configurations with different primary coil transversal cross-section areas A_p was obtained. In this paper, transformers are always energized to the primary winding.

Table 1. Transformers data

Transformer	1		2	
Nominal power (VA)	1 200		1 200	
Nominal voltage (V)	230		230	
Core type	UI 132		UI 132	
Limb width/packet thickness (mm)	44/46		44/46	
Material losses, sheet thickness	M 165-35 S		M 165-35 S	
Coil	inner	outer	inner	outer
Height of winding (mm)	2×125	2×125	2×125	2×125
Turns (-)	320	320	320	320
Wire diameter (mm)	1.25	1.25	1.9	1.9
Coil distance from limb (mm)	0.7−4.5	14−17.5	1.7−7.2	9.5−15
*Derived from wire resistance	1−5	10−14	2−6.5	8−12

The block scheme of measurement is shown in Fig. 1. The positioning table was used to move the transversal Hall probe in the coil gap. The waveforms of primary voltage, current and axial component of the stray field were measured during transformer energizing. The remanent flux before the energizing instant was generated by the transformer switch-off angle.

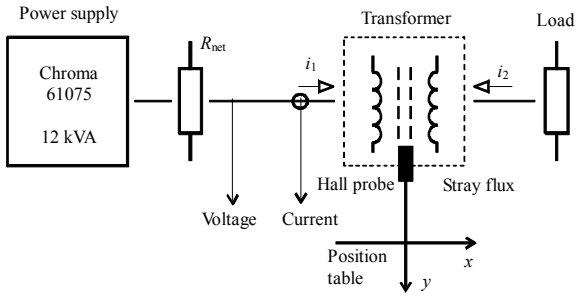

Fig. 1. The measurement setup

Figure 2 shows the experimental results obtained for the second transformer against the switching angle. The outer winding was used as primary. Two sets of measurements were performed with both polarities of the residual flux ± 0,65 T. These two curves form the boundary to the area of all possible peaks of the inrush current. In reality, when the transformer energizing is uncontrolled, the maximal inrush current can be wherever inside this area depending on the actual switch on angle and remanent flux. The worst case occurs at $\theta = 0$ °, B_r = *-max* or $\theta = 180$ °, B_r = *+max*. The theoretical calculation (7) determines only these maximal values. The tested transformers have maximal inrush current 15–30 pu.

The nominal current is represented in both polarities by two black horizontal lines.

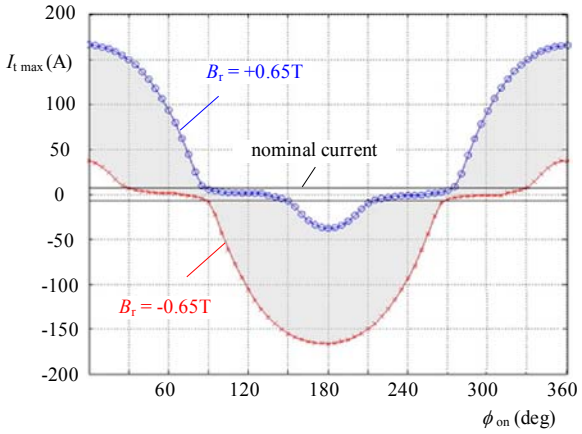

Fig. 2. Peak value of the first cycle of inrush current, Transformer 2, outer coil as primary

The two graphs in Fig. 3 show a screen shot of stray field time animation.

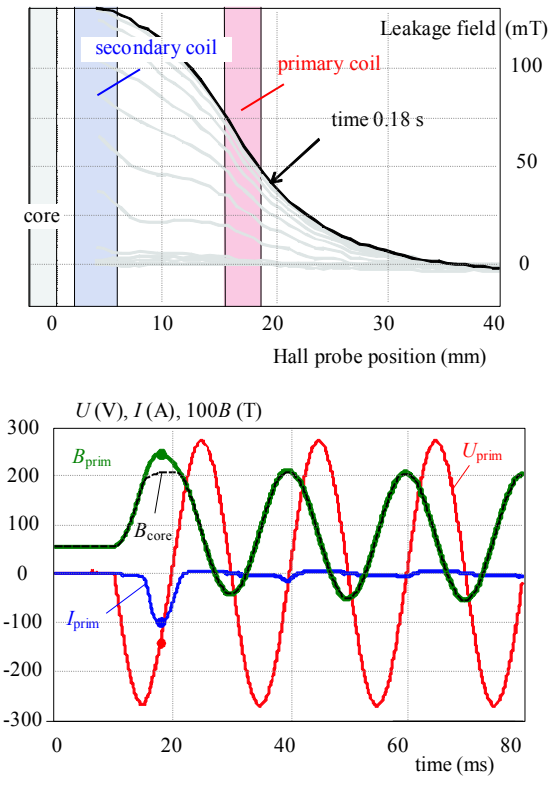

Fig. 3. Stray flux of Transformer 1, radial measurement in the middle of coils

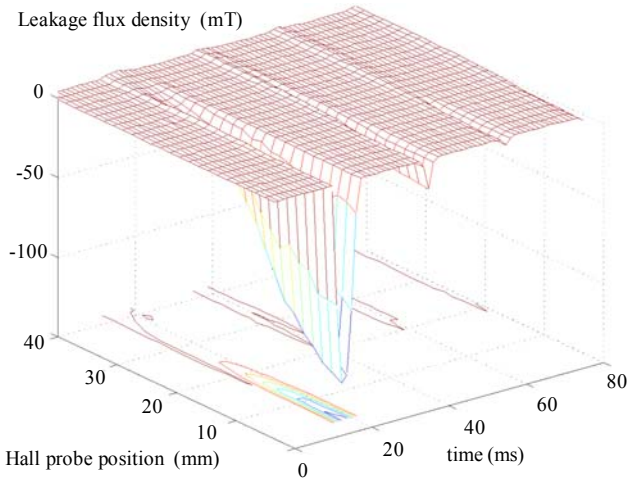

Fig. 4. Magnetic field in coil gap during inrush current, Transformer 2, no-load

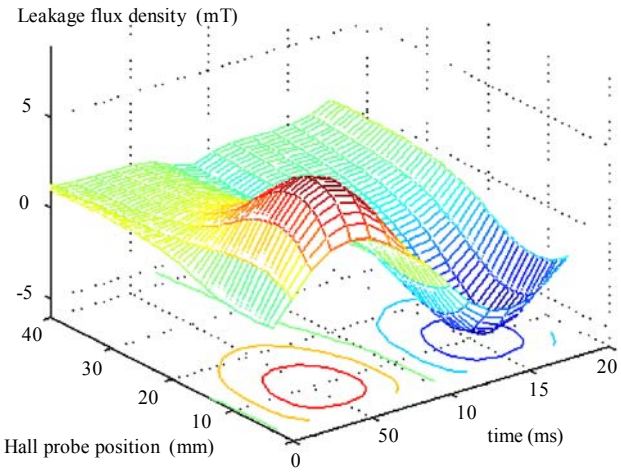

Fig. 5. Magnetic field in coil gap during inrush current, Transformer 2, nominal resistive load

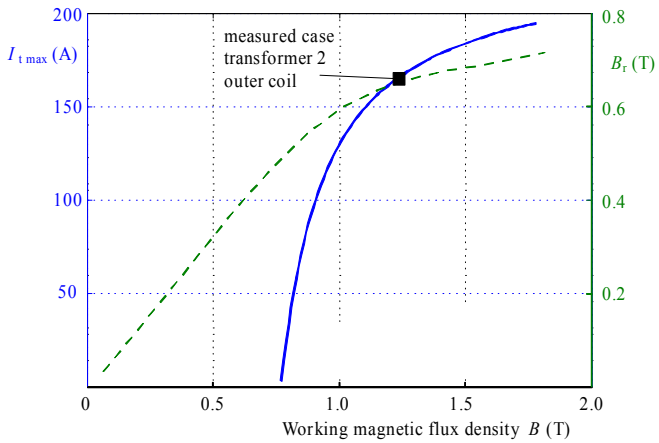

Fig. 8. The dependence of inrush current on working magnetic flux density, Transformer 2, outer coil as primary winding

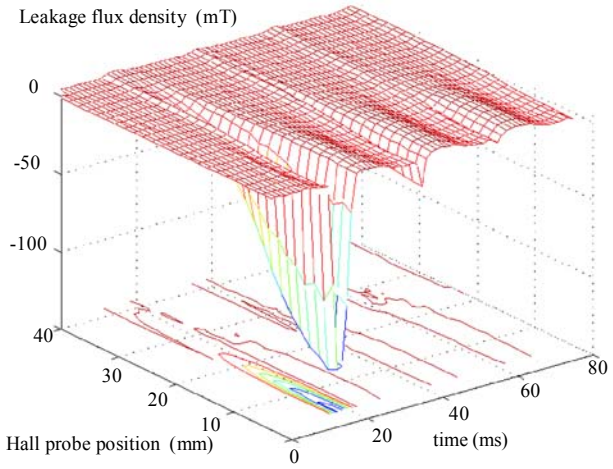

Fig. 6. Magnetic filed in coil gap at steady operation state, Transformer 2, nominal resistive load

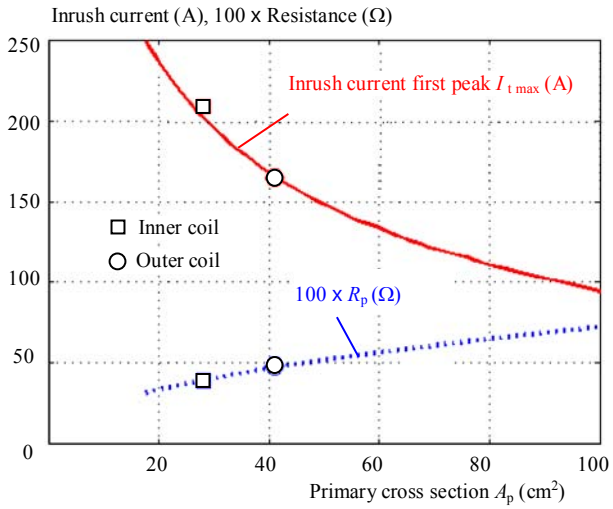

Fig. 7. The variation of inrush current vs. primary coil cross section area, Transformer 2

Grey lines in the upper graph are stray field curves for different time points. The black curve indicates field for the maximal peak of inrush current which is marked by circles in the bottom graph. The flux density in the transformer core B_{core} was derived from the flux density of the primary winding B_{prim} with regard to the leakage field B_{leak} measured by the Hall probe

$$B_{core} = B_{prim} - \int B_{leak}(y)\frac{4(y+a)}{A_c}dy\,, \qquad (9)$$

where y - is the distance of Hall probe from the core and a is the core limb width. The transformer core has square cross-section in this case.

The distribution of the magnetic field density in time and distance during the transformer energizing is shown in Fig. 4, which shows the situation with a non-loaded transformer, and in Fig. 5, which shows the situation for a

transformer with a nominal resistive load. In these two figures, the primary winding is outer coil.

The peaks of the magnetic field from the magnetizing current created by the primary coil are the most distinctive in these figures. The waveform shape corresponds to the waveform of the inrush current. The magnitude should be damped in the primary coil to zero, but the measured field close to the coil is deformed because of the air gap for the Hall probe. Outside the winding, the field has reverse polarity with much smaller magnitude.

The transformer load current creates leakage field in the space between the primary and the secondary coil. For concentric primary and secondary windings which have equal heights the leakage field is predominantly axial. The theoretical leakage field pattern is trapezoidal [3] with magnitude $B = \mu_0 \sqrt{2} In / l$, where I is current and l is the height of the winding. The measured leakage field is rather dome-shaped, located between the primary and the secondary coil with magnitude of 60 % of the theoretical value, see Fig. 6. The leakage field has phase shift $\pi/2$ from the magnetizing field and its magnitude is 20 times weaker than the maximal first peak of the magnetizing current closest to the core.

The measurements are compared to the theoretical values given by numerical model according to equations (1) to (6) in Table 2. Fig. 7 shows graphical representation model results for transformer 2. The inrush current hyperbolically drops as the primary cross-section area increases. The resistance curve is calculated from the geometrical size of the coil. The coil resistance has square root behaviour towards the coil cross-section area.

Table 2. Comparison of theoretical and measured inrush current, U = 190 V, B = 1.24 *T*, R_{net} = 0.33 Ω

Transformer	A_p (m^2)	R_p (Ω)	Theory I_{max} (A)	Meas. I_{max} (A)	B_{stray} peak (mT)
1: inner	2.5×10^{-3}	0.88	155	150	120
1: outer	$4.\times10^{-3}$	1.18	113	103	133
2: inner	2.8×10^{-3}	0.39	209	209	172
2: outer	4.1×10^{-3}	0.48	166	165	200

Figure 8. shows the influence of the working magnetic flux on the inrush current obtained form numerical model for transformer 2 with the outer winding as the primary. The dashed line gives information of the remanent magnetic flux density, which is an important part of equation (2). The remanent flux density was measured at the steady working state with no-load condition.

There is no inrush current for working magnetic flux lower than 0.76 T because the maximal flux during the transformer energizing is lower than the saturation point of the core material. The inrush current quickly increases when the working flux exceeds the saturation point, but for high values the inrush current is restricted by the primary circuit impedance and the air core inductance of the primary winding.

4 CONCLUSIONS

The measurements confirm the role of the primary stray field for the inrush current limitation. The results of theoretical model correspond well to the reality when the primary circuit impedance is taken in account. The usage of outer winding as the primary or even the increase primary diameter through spacers is recommended for decreasing of the transformer inrush current.

Acknowledgement

This work was supported by grant GAČR 102/08/P453 "Transformer inrush current suppression".

REFERENCES

[1] LEÓN, F. – GLADSTONE, B. – VEEN, M. Transformer Based Solutions to Power Quality Problems, Proc. 14th Int. Power Quality Conf. (2001)

[2] STEURER, M. – FRÖHLICH, K.: The Impact of Inrush Currents on the Mechanical Stress of High Voltage Power Transformer Coils, IEEE Trans. On Power Delivery, vol. **17**, no. 1 (2002), pp. 155-160

[3] KULKARNI, S.V. – KHAPARDE, S. A. Transformer Engineering, Design and Practice. Marcel Dekker, Inc. (2004)

[4] GIRGIS, R. S. – TENYENHUIS, E. G. Characteristics of Inrush Current of Present Designs of Power Transformers, Power Engineering Society General Meeting (2007), IEEE

[5] WANG, Y. – ABDULSALAM, S.G. – XU, W. Analytical Formula to Estimate the Maximum Inrush Current, IEEE Trans. On Power Delivery, vol. 23, is. 2 (2008) 1266–1268

[6] VANTI, M.G. – BERTOLI, S.L. – CABRAL, S.H.L. – GERENT, A.G. – KUO, P.P. Semi-analytic Solution for a Simple Model of Inrush Currents in Transformers, IEEE Trans. on Magnetics, vol. 44, is. 6 (2008) 1270–1273

[7] SAINZ, L. – CORCOLES, F. – PEDRA, K. – GUASCH, L. Theoretical Calculation of Inrush Currents in Three- and Five-Legged Core Transformers, IEEE Trans. on Power Delivery, vol. 22, is. 2 (2007) 986–995

[8] THEOCHARIS, A.D. – MILIAS-ARGITIS, J. – ZACHARIAS, Th. Single-phase transformer model including magnetic hysteresis and eddy currents, Elect. Eng. Vol. 90 (2008) 229-241

[9] CHENG, Ch. K. – CHEN, J. F. – LIANG, T. J. – CHEN, S. D. Transformer design with consideration of restrained inrush current, Int J Power Energy Syst. **28** (2006), 102–108

[10] NOVAK, M. Transient Phenomenon During Transformer Energizing – Methods of Inrush Current Suppression, [Ph.D. Thesis] Tech. Univ. of Liberec, 2003.

Received 30 September 2010